

ON NON-OHMIC CONDUCTION AND THE THRESHOLD CHARACTERISTICS OF A BULK-TYPE SWITCHING DEVICE BASED ON THE CHALCOGENIDE GLASSY SEMICONDUCTOR $As_{0.40}Se_{0.30}Te_{0.30}$

E. MÁRQUEZ, P. VILLARES and R. JIMÉNEZ-GARAY

Departamento de Física, Facultad de Ciencias, Universidad de Cádiz, Apartado 40, Puerto Real, Cádiz, Spain

Received 20 July 1987

Revised manuscript received 8 October 1987

The threshold characteristics of a switching device, based on a bulk semiconducting glass sample of composition $As_{0.40}Se_{0.30}Te_{0.30}$, have been examined. The experimental results are discussed in terms of the thermal breakdown model. The relationship between switching delay time and applied voltage is close to that predicted for the limiting case called impulse thermal breakdown. On the other hand, the dependence of threshold voltage on temperature correctly fits the one corresponding to steady-state thermal breakdown, confirming the fundamentally thermal nature of the electrical switching phenomenon. A non-ohmic process has been observed in the glass alloy under study (there are some signs of a space-charge limited current-type non-ohmic effect), although it does not play an important role in the switching effect. The weak field ohmic resistance-temperature characteristics are of the Arrhenius-type, an activation energy for the electrical conduction process of approximately 0.5 eV having been found. Lastly, the complete thermal balance equation has been numerically solved, and the results show good agreement with the experimental values.

1. Introduction

In all semiconductors or insulators, conditions may occur in which the self-generated Joule heat exceeds the capacity of the system to dissipate it. The current increases with temperature, which leads to more Joule self-heating and the consequent thermal runaway. Chalcogenide glassy semiconductors have large negative temperature coefficients of electrical resistivity and low thermal conductivities, so thermal runaway must always be considered as a possible breakdown mechanism in high electric fields. Even if it is not the dominant mechanism which gives rise to the switching process, thermal effects are likely to be present and their influence must be understood [1,2].

In the present paper, the switching effect observed in the bulk samples of composition $As_{0.40}Se_{0.30}Te_{0.30}$ is considered to be due basically to a thermal breakdown mechanism [3–9]. For this reason, the material has been systematically

characterized in terms of the thermal runaway process; in order to do this, the switching properties have been compared to the functional forms for the proposed mechanism. The current-voltage characteristics in the high-resistance state, or OFF-state, have been experimentally determined, to find the dependence of resistance on voltage, indicating the presence of non-ohmic electronic processes [10–13]; the relationship between low-voltage ohmic resistance and temperature has also been studied.

The new features of this basically thermal analysis are:

(1) The study of the relationship between switching delay time and applied voltage, at different ambient temperatures, comparing the phenomenological dependence found with that predicted by the proposed physical model (heat flow is considered to be parallel to the current).

(2) The accurate determination of the threshold voltage or minimum switching voltage, by extrapo-

lation to $t_0 = \infty$, from delay time-applied voltage characteristics, and the study of the dependence of said threshold voltage on ambient temperature.

(3) The detailed consideration of non-ohmic electronic effects on the analysis, to determine their degree of cooperation in the switching process (the non-ohmic processes are presented, although those associated with Joule self-heating are more important).

(4) In order to enrich the analysis, the energy balance equation has been numerically solved (without suppressing any of its terms), this being something unusual in this kind of study.

In this way, a more complete and precise revision of the switching properties of bulk chalcogenide glassy semiconductors has been attempted. The samples of considerable thickness, i.e., greater than 100 μm , have been studied much less than thin films.

Several researchers have studied the As–Se–Te chalcogenide glassy system [14–18], which has been found to have very stable switching characteristics, as its elements are electrochemically similar (the phenomenon of electrolysis in the low-resistance state, or ON-state, is considerably reduced [19]). However, detailed analyses of the different switching properties, in bulk samples of this glassy system, are scarce. In an attempt to complete the existing information on the As–Se–Te system, the semiconducting glassy alloy $As_{0.40}Se_{0.30}Te_{0.30}$ has been studied.

2. Experimental procedure

2.1. Preparation of the material

The glassy material was synthesized following the melt-quench method. The raw materials As, Se and Te were of 99.999% purity, and were ground and mixed homogeneously in adequate proportions to obtain a total weight of 7 g. The mixture was introduced into a quartz tube, which was repeatedly filled with helium and emptied. The tube was then sealed using an oxiacetilenic blow-lamp, in order to avoid oxidation.

The ampoule containing the mixture was put into a furnace at a temperature of 650 °C for 72 h.

Furthermore, this ampoule was continuously turned at $\frac{1}{3}$ rpm, to ensure homogenization of the material. The preparation process ended with quenching in an icewater bath. The alloy was taken out of the ampoule in one piece, using a corrosive hydrofluoric acid–hydrogen peroxide solution.

2.2. Structural characterization of the material and preparation of the switching device

The non-crystalline character of the ingot was checked by X-ray diffraction analysis (Siemens D500). The X-ray diffraction patterns did not exhibit the well-defined peaks which signal the presence of crystalline residues. On the other hand, the differential scanning calorimetric analysis (DSC-Rigaku, model CN8059D2) confirmed the glassy nature of the material. The glass transition temperature of the alloy under study is approximately 133 °C (the heating rate used to obtain the DSC curve was 20 °C/min).

The samples, in the shape of thick slices, were inlaid in an epoxy-type resin; the bases were finished with alumina powder (0.3 and 0.05 μm grain size). In this way mirror-like surfaces, which allow good electrical contact, were obtained. For the preparation of the bulk switching device, silver paint was used as electrode material. To complete the sandwich-type device, two thin copper discs were added, to which the conducting wires were soldered. The bulk glass sample used as active material of the device was approximately 3.0 mm in diameter and about 1.0 mm thick.

2.3. Measurements with rectangular voltage pulses

In order to determine the OFF-state current-voltage characteristics, and the relationship between switching voltage and the corresponding delay time, rectangular voltage pulses of increasing amplitude were used, with a width of 50 s and an interval, which allowed the sample to cool down to ambient temperature, after electrical excitation. A memory oscilloscope (Trio, model 1650B) was used to measure the switching delay times. Besides, it was not necessary to reach current values higher than 1 mA to experimentally de-

termine these delay times, as the time derivative of the current for lower values was confirmed as being very high; so at those current levels, the tangent line in the current-time characteristics is approximately vertical. The temperature interval analyzed is between room temperature and about 40 °C below the glass transition temperature of the alloy. A temperature controller of $\pm 0.2^\circ\text{C}$ precision (OMRON, model ESK, type PID), was used to regulate the ambient temperature in the experiments.

3. Thermal breakdown

Considering that the only significant loss process is thermal conduction, the energy balance equation is given by

$$C_v \, dT/dt - \text{div}(K_t(T)\text{grad}T) = \sigma(E, T)E^2, \quad (1)$$

where C_v is specific heat per volume unit, σ is electrical conductivity and K_t is thermal conductivity. This is the basic equation in the thermal breakdown process. Since σ and K_t are temperature dependent (the former strongly so) and, in addition, σ may depend on the field, even approximative analytic solutions of eq. (1) are not possible for any but the simplest boundary conditions.

The problem of solving the thermal balance equation can be approached in three different ways:

- (1) Determination of steady-state thermal breakdown, which involves ignoring the time derivative in eq. (1).
- (2) Determination of impulse thermal breakdown by ignoring the heat conduction term in eq. (1).
- (3) Numerical solutions of eq. (1) for simple cases.

3.1. Steady-state thermal breakdown

The bulk glassy semiconductor is considered to be homogeneous, cylindrical (thickness, d , and area of cross-section, S), with a thick covering of insulator material on the lateral surface, which

constitutes a strong thermal impediment between the glassy semiconductor and the ambient medium. If the z direction is taken perpendicular to the electrode surfaces, then it can be supposed approximately that all heat flow will be in the z direction. With these restrictions, eq. (1) is reduced to

$$\partial/\partial z(K_t \partial T/\partial z) + \sigma(\partial V/\partial z)^2 = 0. \quad (2)$$

It is assumed that z is measured from the central plane, at which the temperature is by symmetry a maximum T_m . By introducing the electrical continuity equation, $\partial/\partial z(\sigma \partial V/\partial z) = 0$, eq. (2) changes to

$$\partial/\partial z(K_t \partial T/\partial z) - (I/S) \partial V/\partial z = 0. \quad (3)$$

Integrating eq. (3) from the centre to a variable plane, the result is

$$IV/S = \int_0^z \partial/\partial z(K_t \partial T/\partial z) \, dz = K_t \partial T/\partial z, \quad (4)$$

since $\partial T/\partial z = 0$ at $z = 0$. Integrating eq. (4) from the centre to the electrode where, according to the notation used, $V = V_0/2$ and $T = T_1$ ($V = 0$ in the central plane, so V_0 is the interelectrode voltage), one arrives at

$$V_0^2 = 8 \int_{T_1}^{T_m} (K_t/\sigma) \, dT. \quad (5)$$

In order to make progress, a further assumption is required. It is supposed that a constant external thermal conductance, λ , exists such that the heat lost, per area unit and time unit, by the glassy semiconductor surface at T_1 , to ambient temperature T_0 , is given by $\lambda(T_1 - T_0)$. That is to say, the usual Newtonian expression is used to formulate the corresponding heat dissipation. In the steady state, it is verified that

$$(I/2S)V_0 = \lambda(T_1 - T_0), \quad (6)$$

since approximately half of the heat generated by the current will be lost through each electrode surface. By combining eqs. (3) and (6) and integrating, one obtains

$$K_t \partial T/\partial z - 2\lambda(T_1 - T_0)V/V_0 = 0, \quad (7)$$

as it is considered that $V = 0$ when $\partial T/\partial z = 0$.

Integrating eq. (7) from the centre to the electrode, the following expression results

$$\lambda(T_1 - T_0)d/V_0 = \int_{T_1}^{T_m} \frac{K_V dT}{\left[\int_T^{T_m} (2K_V/\sigma) dT \right]^{1/2}}, \quad (8)$$

Equations (5) and (8) determine the thermal breakdown process.

3.2. Impulse thermal breakdown

The opposite limiting case to that of a steady state, is one in which the thermal conduction process plays a negligible role. The fundamental equation (1) then becomes

$$C_v dT/dt = \sigma(E, T)E^2, \quad (9)$$

which determines the critical conditions for impulse thermal breakdown. If the time dependence of the applied voltage pulse and the dependence of electrical conductivity on voltage and temperature are known, eq. (9) can be integrated, giving way to the relationship between switching voltage and delay time, t_0 , or time required for T_m to exceed the critical temperature $T_{m,c}$. This is the highest temperature at $z = 0$, for a thermal stability situation, and it is asymptotically reached when the threshold voltage, $V_{0,th}$, is applied.

4. Experimental results and discussion

4.1. Dependence of electrical conductance on voltage and temperature

To establish the electrical conduction mechanism in high fields, the $I(t=0)$ vs. V_0 characteristics have been experimentally determined, thus excluding the Joule self-heating effects associated with electrical excitation (the method used to determine the current at instant $t=0$ consists of fitting the different values of the current, corresponding to different instants, to the functional dependence belonging to this type of non-crystalline materials [7,10]. In this way it is possible to find the dependence of isothermal static resistance

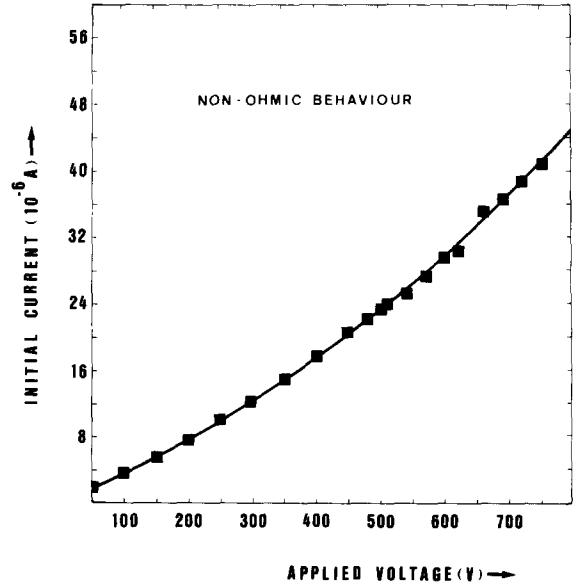


Fig. 1. Non-linear $I(t=0) - V_0$ characteristics, in the OFF-state and at room temperature.

on applied voltage. Figure 1 shows the $I(t=0) - V_0$ characteristics for the semiconducting glassy alloy $As_{0.40}Se_{0.30}Te_{0.30}$, with a sandwich-type electrode configuration and at room temperature (similar initial current–voltage characteristics are found at higher ambient temperatures [20]). It may be observed that at low voltages, electrical conduction is ohmic, while at high voltages the behaviour of the device is non-linear. The functional form which the experimental values fit is

$$I(V_0) = G_\Omega V_0 \exp(V_0/V_1), \quad (10)$$

G_Ω being ohmic conductance, and V_1 being a parameter which gives the value of the voltage at which the non-ohmic effects, derived from some process of an electronic nature, begin to be relevant. From eq. (10) one deduces the dependence between electrical conductance and voltage, $G(V_0) = G_\Omega \exp(V_0/V_1)$. Figure 2 shows $\ln R(V_0)$ vs. V_0 at room temperature, and in it the good agreement between the experimental values and the indicated functional dependence may be observed. The values obtained for V_1 and G_Ω by linear regression analysis are 1533 V and $4 \times 10^{-8} \Omega^{-1}$ ($r = 0.995$).

Dependence (10) may correspond to the single-carrier space-charge limited current flow

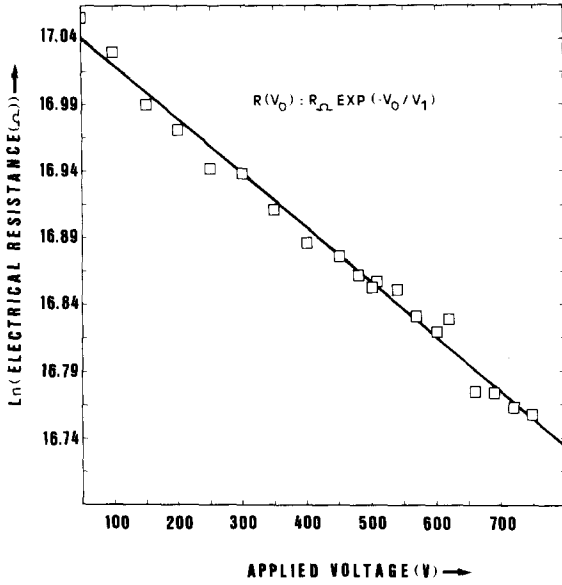


Fig. 2. Representation of $\ln R$ vs. V_0 at room temperature.

(SCLC) model, with a Fermi level in a uniform trap distribution [11], and the model corresponding to field-assisted carrier release from shallow trapping levels. In this mechanism, at intermediate voltages, the electrical conductance expression is of the type [12]

$$G(V_0) = G_\Omega \sinh(rq_e V_0 / k_B T_0 d) / (rq_e V_0 / k_B T_0 d), \quad (11)$$

r being the effective radius of the trapping center, k_B the Boltzmann constant and q_e the electron charge. This expression, at sufficiently high voltages, and considering a square-well type trapping center, becomes relationship (10) [12]. In this conduction mechanism, the expression of V_1 is as follows:

$$V_1 = k_B T_0 d / q_e a(T_0) \quad (12)$$

in which $a(T_0)$ is the temperature-dependent activation distance, and relationship (10) is valid for voltage values higher than parameter V_1 (according to this mechanism, transition to ohmic behaviour takes place at voltages $V_0 \leq V_1$). However, the values of V_1 determined by adjusting the experimental data to dependence (10) are remarkably higher than the applied voltages, which

is inconsistent with the necessary conditions for the application of eq. (10).

On the other hand, when the experimental values are adjusted to relationship (11), one finds a worse fit in comparison to that found for functional dependence (10); i.e., the electrical conductance expression corresponding to the conduction model associated with carrier release from shallow traps at intermediate voltages is not valid either. Besides, going back to expression (12), as the experimentally-found dependence between V_1 and T_0 is $V_1 \propto T_0$ [20], the existence of an activation length dependent on temperature, as predicted by the carrier release model, would not be possible under these conditions. However, this experimentally-determined V_1 - T_0 dependence agrees with the one for the SCLC model. Also, the experimentally determined value of $a(T_0)$ in the present work is approximately 178 Å, and this is much higher than those quoted in the bibliography (the highest is 40 Å, and corresponds to the lowest of the temperatures, $T_0 \approx 60$ K, as $a(T_0)$ decreases when temperature increases) [12]. To continue with the discussion in terms of the single-carrier SCLC mechanism, if the distribution of localized states in the mobility gap is uniform, the V_1 expression for this process is of the type [11]

$$V_1 = q_e N_t k_B t_0 d^2 / \epsilon, \quad (13)$$

N_t being the trap density and ϵ the dielectric constant. From the proportionality constant corresponding to the experimentally found relationship between V_1 and T_0 , whose value is 5.05 V K^{-1} [20], and bearing in mind that $\epsilon = 17.7$ (CGS units) [21], one finds that $N_t = 7.2 \times 10^{14} \text{ eV}^{-1} \text{ cm}^{-3}$.

As a consequence of the analysis carried out, it seems reasonable to think that an SCLC-type electronic process is responsible for the non-ohmic effects observed. However, in order to confirm the validity of this conduction model, it would be desirable to study the dependence between V_1 and the thickness (according to the SCLC process, the relationship ought to be of the type $V_1 \propto d^2$).

The measurements of ohmic resistance at different temperatures are analyzed forthwith. The experimental values adequately fit ($r = 0.992$) the

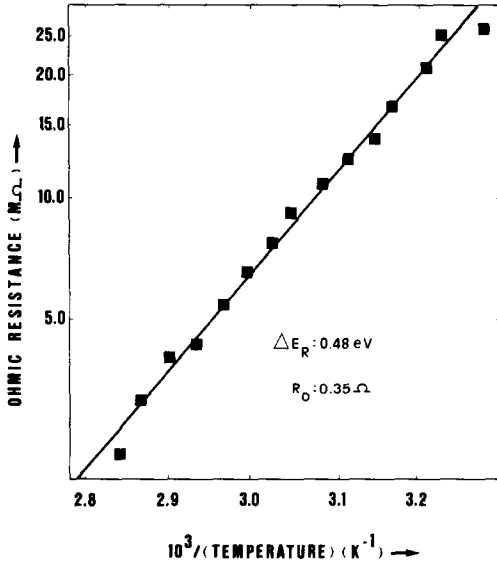


Fig. 3. Ohmic resistance, R_Ω , versus temperature inverse (semi-logarithmic scale).

well-known Arrhenius-type relationship, corresponding to thermally activated mechanisms

$$R_\Omega(T_0) = R_0 \exp(\Delta E_R / k_B T_0), \quad (14)$$

R_0 being a pre-exponential factor, and ΔE_R being the activation energy for the electrical conduction process, determined from these measurements of the weak field electrical resistance, at different temperatures. In fig. 3, R_Ω vs. $1/T_0$ is represented at semilogarithmic scale; one deduces from the slope that $\Delta E_R = 0.48$ eV and the intersection with the y axis takes place at $R_0 = 0.35 \Omega$. According to the value found for ΔE_R and to the value of the pre-exponential factor associated with electrical conductivity, $\sigma_0 \approx 100 \Omega^{-1} \text{ cm}^{-1}$, it may be deduced that electrical conduction in the weak field is due basically to carriers excited beyond the mobility shoulders into non-localized or extended states (the value of σ_0 has been determined from the value of R_0 , considering the values of S and d in the sample, approximately 0.20 mm^2 and 0.7 mm , since in this case different dimensions from those in the switching device have been used) [22]. Electrical conductivity of the glassy alloy under study at 20°C is approximately $5.6 \times 10^{-7} \Omega^{-1} \text{ cm}^{-1}$.

In the following sections, relationship (14) will be used to find the expression of delay time as a function of the applied voltage, and the temperature dependence of the threshold voltage.

4.2. Delay time-applied voltage characteristics at different temperatures

Taking eq. (9), corresponding to impulse thermal breakdown, and bearing in mind that the electrical excitation of the glass sample, whose ohmic resistance verifies relationship (14), is carried out by applying rectangular voltage pulses, it turns out that

$$C_v dT/dt = (\sigma_0/d^2) \exp(-\Delta E/k_B T) V_0^2. \quad (15)$$

in the first approximation, the above-mentioned non-ohmic electronic effects are not introduced, as the applied voltage pulses were all of amplitudes below 1 KV, and consequently lower than V_1 . That is to say, although the non-ohmic processes are presented, their contribution to the switching phenomenon is less relevant in comparison to the thermal-type effects. The time interval, t_D , necessary for the critical temperature, $T_{m,c}$, to be reached, is given by

$$\int_{T_0}^{T_{m,c}} \exp(\Delta E/k_B T) dT = \sigma_0 V_0^2 t_D / d^2 C_v. \quad (16)$$

Since $\Delta E \gg k_B T$, the integration may be done approximately, resulting in

$$t_D = S d C_v k_B T_0^2 R_\Omega(T_0) / V_0^2 \Delta E = A_t(T_0) / V_0^2. \quad (17)$$

On the other hand, the relationship that the experimental values fit is of the form [23,24]

$$t_D = A_t(T_0) / (V_0 - V_{0,th})^2. \quad (18)$$

Figure 4 shows the current versus time curves (the temperature for this experiment was approximately 67°C), from which the different delay times were evaluated. In addition, fig. 5 shows V_0 vs. $t_D^{-1/2}$, for some of the temperatures studied. Therefore, the slope in this representation is $A_t^{1/2}$ and the intersection with the y axis is $V_{0,th}$ (switching voltage whose delay time is infinite). It may be observed that, as the temperature increases, both $V_{0,th}$ and A_t decrease. Furthermore, the represen-

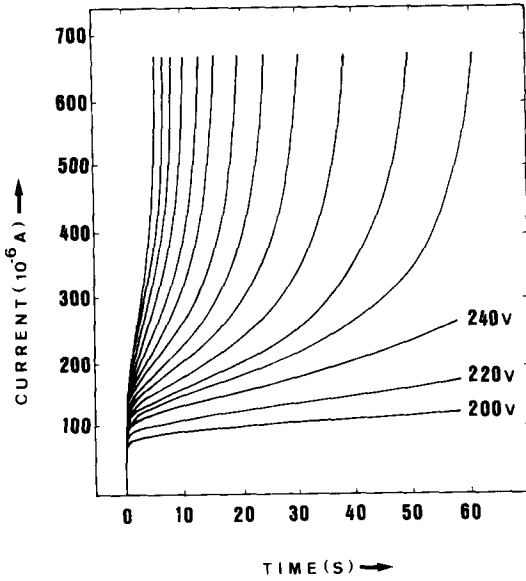


Fig. 4. Current-time characteristics corresponding to different applied voltages (the curves without any indication as to voltage, correspond to voltage values increased in 10 V at a time, i.e., the first one is 250 V and the last one is 360 V).

tation of V_0 vs. t_D has been inserted as an illustration in fig. 5.

The empirical relationship (18) coincides with the expression of delay time as a function of applied voltage, corresponding to impulse thermal breakdown, when the pulse amplitude is considerably higher than $V_{0,th}$. This fact is evidence in favour of the validity of the thermal breakdown theory, as the basis of the explanation of the switching phenomenon in the bulk sample of composition $As_{0.40}Se_{0.30}Te_{0.30}$. On the other hand, parameter A_t (determined by fitting the experimental points to functional dependence (18)) is represented versus $T_0^2 R_D(T_0)$ (fig. 6). According to eq. (17), the relationship must be linear, and the expression of the slope, $C_v k_B S d / \Delta E$. Indeed, the experimental results show good agreement with this relationship ($r = 0.993$) and the value of the slope is $0.63 \times 10^{-6} \text{ J K}^{-2}$. Considering that the value of C_v in this type of glassy materials is approximately $1 \text{ J cm}^{-3} \text{ K}^{-1}$ [25], one deduces that the activation energy determined by A_t , ΔE_A , verifies that $\Delta E_A \approx \Delta E_R$, also confirming the consistency of the switching model proposed.

4.3. Variation of threshold voltage with ambient temperature

The solution of eqs. (5) and (8) will now be obtained, for the case in which the dependence of electrical conductivity on temperature is that expressed by eq. (14) (thermal conductivity is assumed to be independent of temperature). With these restrictions, eqs. (5) and (8) can be written in terms of dimensionless quantities as follows:

$$(c/v)(1/x_1 - 1/x_0) = \int_{x_{m,c}}^{x_1} \frac{dx}{x^2 \left[\int_{x_{m,c}}^x (\exp(x)/x^2) dx \right]^{1/2}}, \quad (19)$$

and

$$v^2 = \int_{x_{m,c}}^{x_1} (\exp(x)/x^2) dx, \quad (20)$$

where the dimensionless quantities $v =$

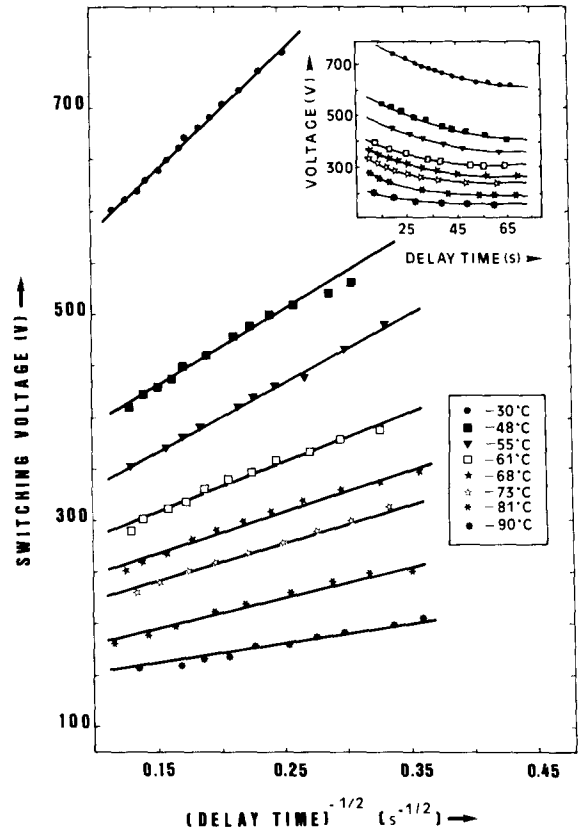


Fig. 5. Representation of V_0 vs. $1/t_D^2$. V_0 vs. t_0 has also been inserted.

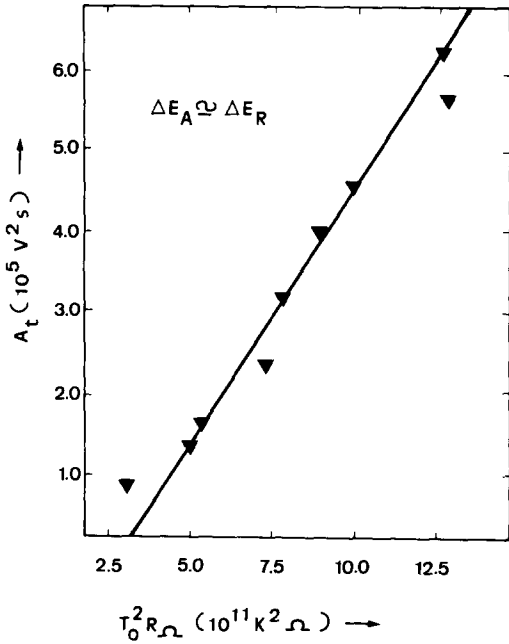


Fig. 6. Representation of $A_t(T_0)$ vs. $T_0^2 R_\Omega(T_0)$.

$V_0(k_B\sigma_0/8 \Delta EK_t)^{1/2}$, $c = \lambda d/2K_t$ and $x = \Delta E/k_B T$ have been introduced (it is understood that subscripts on x imply the same subscript on T). In solving eqs. (19) and (20), two limiting cases arise, that corresponding to very large values of c and the one associated to very small values of c . In the present situation, the value of c is small, 2.5×10^{-2} , as $\lambda \approx 15 \text{ W m}^{-2} \text{ K}^{-1}$ [26] (it is supposed that in the top and bottom boundaries a natural convection process in air takes place) and $K_t \approx 3 \times 10^{-1} \text{ W m}^{-1} \text{ K}^{-1}$ [27]. Although the glass sample may obviously be considered to be of remarkable thickness, from the standpoint of thermal conduction it can be classified, following O'Dwyer's criterium [1], as a "thin sample", as the heat evacuation process on the edges plays the fundamental role (in the other limiting case corresponding to the so-called "thick sample", in which $\lambda d \gg 2K_t$, it is verified that $T_1 = t_0$, i.e., most efficient edge cooling). For the case in which c is very small, the analytic solution of eqs. (19) and (20) gives way to the approximate expression [1].

$$v_{th} = (c/2 e)^{1/2} (1/x_0) \exp(x_0/2), \quad (21)$$

which can be rewritten as

$$V_{0,th} = (\Gamma k_B R_0 / e \Delta E)^{1/2} T_0 \exp(\Delta E / 2k_B T_0), \quad (22)$$

where $\Gamma = 2\lambda S$, i.e., the coefficient of heat transmission by convection of the device.

The experimental values of the threshold voltage, determined by extrapolating to the value $t_D = \infty$, are shown in fig. 7, where the remarkable sensitivity of the threshold voltage to ambient temperature increase may be observed. Figure 8 shows $V_{0,th}/T_0$ vs. $1/T_0$ at a semilogarithmic scale ($r = 0.998$). The activation energy determined from the variation of threshold voltage with ambient temperature, ΔE_v , is 0.46 eV, meaning also that $\Delta E_v \approx \Delta E_R$. The value found for Γ is 0.22 mW K^{-1} , which gives way to a value of λ very close to that considered before, bearing in mind the natural convection process in the bases of the device.

On the other hand, from eq. (22) one obtains the relationship

$$V_{0,th}^2 = \Gamma k_B T_0^2 R_\Omega(T_0) / e \Delta E. \quad (23)$$

If one takes into account that the strongest dependence of the threshold voltage on temperature is that of the exponential type on the temperature

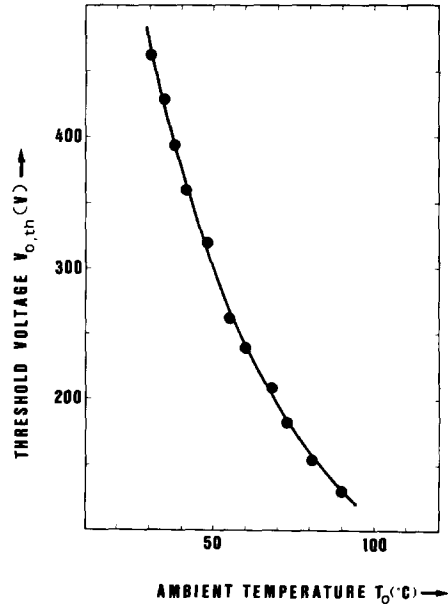


Fig. 7. Threshold voltage ($t_0 = \infty$) versus ambient temperature.

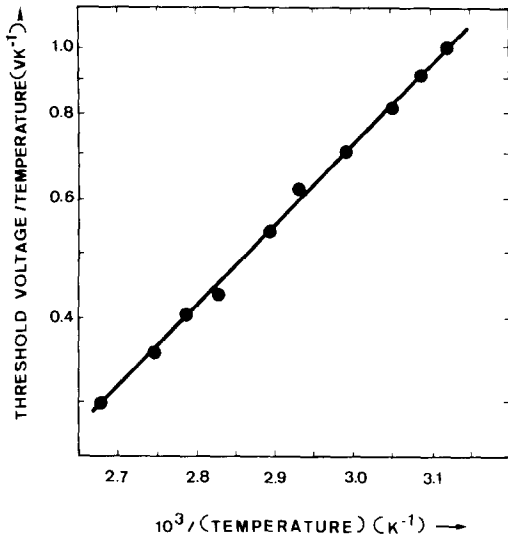


Fig. 8. $V_{0,th}/T_0$ versus $1/T_0$ at semilogarithmic scale. $\Gamma = 0.22$ mW K^{-1} , $\Delta E_v = 0.46$ eV.

inverse contained in the ohmic resistance, eq. (23) can be approximated, without any significant error, to the following expression:

$$V_{0,th}^2 \approx \text{constant} \times R_{\Omega}(T_0). \tag{24}$$

From this equation it is deduced that the threshold initial power, $V_{0,th}^2/R_{\Omega}(T_0)$, is not very sensitive to variations in ambient temperature, in the whole temperature range studied. In fig. 9, $V_{0,th}$ versus $R_{\Omega}(T_0)$ is represented graphically at a log-log scale ($r = 0.996$). The slope is 0.45, that is, there is a 10% difference with the theoretically found value. The average threshold initial power obtained is 8.7 ± 0.9 mW, this value being close to others quoted in the bibliography [7,9,23] for different bulk chalcogenide glassy samples.

4.4. Numerical solution of the thermal balance equation

The types of thermal breakdown, so far considered from a theoretical point of view, correspond to the limiting cases of infinite and infinitesimal time of voltage application. This section expounds the results found by numerically solving the thermal balance equation, without omitting any of its terms. In order to simplify, it is assumed that the temperature distribution in the glass sample is

uniform, so the energy balance equation is, under these conditions, the following:

$$v_0^2/R_{\Omega}(T) = SdC_v \, dT/dt + \Gamma(T - T_0). \tag{25}$$

By solving this equation, one finds the time evolution of the temperature of the glassy sample during electrical stimulation and, therefore, the time dependence of the current. The successive numerical integrations, through which the $T-t$ characteristics are determined for each voltage, have been carried out following the familiar Simpson's rule (the upper limit of the integral is conveniently modified). The values of ΔE_R , R_0 and Γ used when doing the numerical integrations are those obtained experimentally [28].

Figure 10 shows the results of the numerical solution, at an ambient temperature of $55^\circ C$. It may be observed in this figure that when $V_0 = 240$ V, thermal stability is reached; while at other voltages, whose time evolutions of temperature are also represented, the thermal instability which is mainly responsible for the switching process takes place. Analysis of the voltage interval between 240 and 246 V, to determine the threshold voltage more accurately, showed that the minimum voltage at which the switching process originates is 244 V [28]. This numerically obtained value for $V_{0,th}$ is close to the experimentally determined

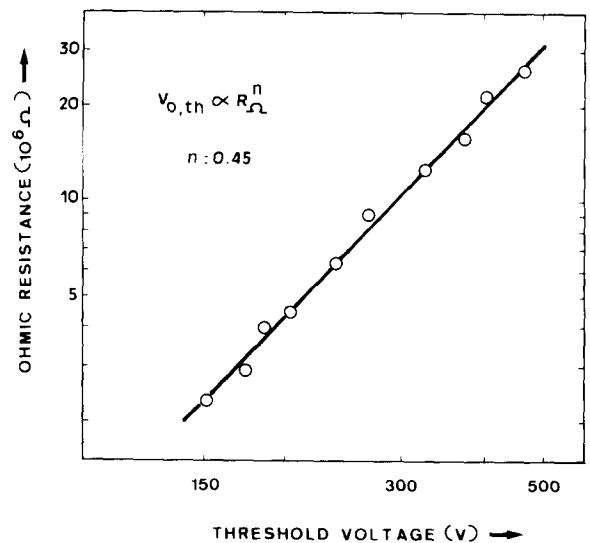


Fig. 9. Representation of ohmic resistance vs. threshold voltage, at log-log scale.

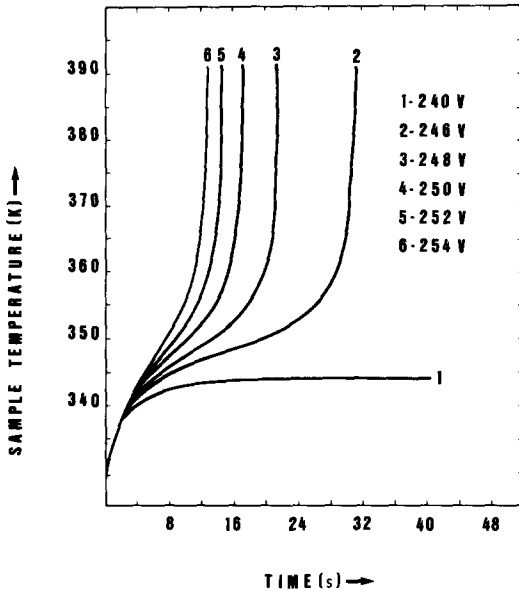


Fig. 10. Time dependences of the temperature of the sample, obtained by numerically solving the complete thermal balance equation, belonging to different voltage values.

value of 264 V (the difference is less than 8%). Therefore, the simplifying hypotheses, considered when expressing the complete thermal balance equation through eq. (24), are reasonable and the validity of the proposed physical model is confirmed once more.

5. Conclusions

The main conclusions which can be deduced from the present paper are the following:

(1) The current–voltage characteristics, without the contribution of Joule self-heating, reveal the presence of non-ohmic effects. According to the experimental evidence presented, non-linear behaviour may be attributed in principle to an SCLC-type electrical conduction mechanism, with a uniform trap distribution. However, thickness scaling experiments must be carried out in order to provide unambiguous evidence of space-charge mechanisms.

(2) The dependence of ohmic resistance on temperature is the one corresponding to thermally

activated processes. The activation energy for electrical conduction has a value of about 0.5 eV, the usual for this type of chalcogenide glassy semiconductors.

(3) The phenomenological dependence between switching delay time and applied voltage is close to the relationship predicted by the case of impulse thermal breakdown, when the applied voltages are much higher than $V_{0,th}$.

(4) The experimentally determined variation of threshold voltage with temperature can be explained considering the limiting case of steady-state thermal breakdown. The relationship found between $V_{0,th}$ and R_{Ω} can also be justified through this theory.

(5) The numerical solutions of the complete thermal balance equation, with the approximative hypotheses mentioned, show good agreement with the experimental results. Furthermore, the time evolution of the temperature of the material, determined by solving the thermal balance equation, shows the positive feedback mechanism which plays an essential role in switching in the analyzed device.

(6) Finally, although a field dependence of electrical resistance has been found, since the value of V_1 is higher than the values of the threshold voltage at different ambient temperatures, it may be concluded that the switching phenomenon observed is a process which is mainly generated by Joule self-heating and the low heat evacuation capacity of the bulk-type switching device under study. In other words, it has been shown that there is clearly a coexistence of thermal and electronic mechanisms, but the cooperation corresponding to non-ohmic conduction is scarcely important; as in the voltage interval in which switching takes place, the heat generation effects in the chalcogenide glassy semiconductor, inherent to electrical conduction, are predominant over the non-ohmic electronic mechanisms that appear in it.

The authors wish to express their gratitude to Aurora Rice for her cooperation in translating the manuscript. They are also grateful to Manuel Domínguez and José Vázquez for their useful contributions.

References

- [1] J.J. O'Dwyer, *The Theory of Dielectric Breakdown of Solids* (Oxford Univ. Press, Oxford, 1964).
- [2] R. Stratton, *Progress in Dielectrics* 3 (1961) 234.
- [3] H. Fritzsche and S.R. Ovshinsky, *J. Non-Cryst. Solids* 4 (1970) 464.
- [4] A.C. Warren, *J. Non-Cryst. Solids* 4 (1970) 613.
- [5] J.M. Robertson and A.E. Owen, *J. Non-Cryst. Solids* 8-10 (1972) 439.
- [6] A.E. Owen, J.M. Robertson and C. Main, *J. Non-Cryst. Solids* 32 (1979) 17.
- [7] E. Márquez, P. Villares and R. Jiménez-Garay, *J. Non-Cryst. Solids* 74 (1985) 195.
- [8] E. Márquez, P. Villares and R. Jiménez-Garay, *Mat. Letters* 5 (1987) 296.
- [9] A. Alegría, A. Arruabarrena and F. Sanz, *J. Non-Cryst. Solids* 58 (1983) 17.
- [10] E. Márquez, P. Villares and R. Jiménez-Garay, *Mat. Letters* 4 (1986) 52.
- [11] M.A. Lampart, *Proc. IRE* 50 (1962) 1782.
- [12] J.M. Marshall and G.R. Miller, *Phil. Mag.* 27 (1973) 1151.
- [13] M. Ieda, G. Sawa and S. Kato, *J. Appl. Phys.* 42 (1971) 3737.
- [14] M. Roilos, *J. Non-Cryst. Solids* 6 (1971) 5.
- [15] M. Roilos, D. Meimaris and K. Zigiris, *J. Non-Cryst. Solids* 7 (1972) 271.
- [16] D.D. Thornburg, *J. Non-Cryst. Solids* 17 (1975) 9.
- [17] M.J. Zope and J.K. Zope, *J. Non-Cryst. Solids* 74 (1985) 47.
- [18] J. Vázquez, E. Márquez, P. Villares and R. Jiménez-Garay, *Mat. Letters* 4 (1986) 360.
- [19] D. Shanefield, *J. Non-Cryst. Solids* 2 (1970) 210.
- [20] E. Márquez, P. Villares and R. Jiménez-Garay, *Mater. Sci. Eng.* 100 (1988) 229.
- [21] B.T. Kolomiets, *Phys. Stat. Sol.* 7 (1964) 359.
- [22] N.F. Mott and E.A. Davis, *Electronic Processes in Non-Crystalline Materials* (Clarendon, Oxford, 1979).
- [23] M. Haro, E. Márquez, L. Esquivias and R. Jiménez-Garay, *J. Non-Cryst. Solids* 81 (1986) 255.
- [24] M. Sugi, S. Iizima, K. Tanaka and M. Kikuchi, *Sol. St. Commun.* 7 (1969) 1805.
- [25] T. Takeda and G. Nogami, *J. Non-Cryst. Solids* 51 (1982) 11.
- [26] F. Kreith and W.Z. Black, *La Transmisión del Calor* (Alhambra, Madrid, 1983).
- [27] W.W. Sheng and C.R. Westgate, *Sol. St. Commun.* 9 (1971) 387.
- [28] E. Márquez, P. Villares and R. Jiménez-Garay, *J. Mater. Sci.* 22 (1987) 4434.